

---

# Tackling Provably Hard Representative Selection via Graph Neural Networks

---

Seyed Mehran Kazemi, Anton Tsitsulin, Hossein Esfandiari, MohammadHossein Bateni,  
Deepak Ramachandran, Bryan Perozzi, and Vahab Mirrokni

Google Research

{mehrankazemi, tsitsulin, esfandiari, bateni,  
ramachandrand, hubris, mirrokni}@google.com

## Abstract

*Representative selection* (RS) is the problem of finding a small subset of exemplars from an unlabeled dataset, and has numerous applications in summarization, active learning, data compression and many other domains. In this paper, we focus on finding representatives that optimize the accuracy of a model trained on the selected representatives. We study RS for data represented as *attributed graphs*. We develop *RS-GNN*, a representation learning-based **RS** model based on **Graph Neural Networks**. Empirically, we demonstrate the effectiveness of RS-GNN on problems with predefined graph structures as well as problems with graphs induced from node feature similarities, by showing that RS-GNN achieves significant improvements over established baselines that optimize surrogate functions. Theoretically, we establish a new hardness result for RS by proving that RS is hard to approximate in polynomial time within any reasonable factor, which implies a significant gap between the optimum solution of widely-used surrogate functions and the actual accuracy of the model, and provides justification for the superiority of representation learning-based approaches such as RS-GNN over surrogate functions.

## 1 Introduction

In the age of massive data, having access to tools that can select exemplar data points representative of an entire dataset can speed up machine learning deployments and make them more resource efficient. Over the years, several representative selection (RS) algorithms have been developed and found applications in various domains [66, 32, 18, 38, 25]. In this paper, we study the RS problem for attributed graphs, where we are given features for each data point and a graph context specifying the connections between them. RS for attributed graphs has several applications including content summarization (e.g., where the input is a graph of content items such as documents, videos, etc. and feature vectors such as text or video embeddings that describe the content), one-shot active learning (e.g., selecting a subset of the nodes to be labeled when obtaining labels is expensive and training models is also expensive), data compression/distillation (e.g., shrinking the size of a graph for faster inference in downstream applications), and several others. Despite its extensive applicability, RS for attributed graphs has remained an under-explored problem in the literature.

In this paper, we develop RS-GNN: a learning-based model for **Representatives Selection via Graph Neural Networks**. We first demonstrate the effectiveness of RS-GNN for selecting representative nodes from datasets with a natural graph representation i.e. where edges may be specified by some natural property of the data (e.g. paper citations). Then, we extend the applicability of RS-GNN to datasets where a natural graph is not readily available, by showing that it can select high-quality representatives even when applied on a similarity graph of node features. We conduct experiments on a suite of eight datasets with different sizes and properties, and in both settings where we have

access to a graph structure and we do not. We find that our model provides significant improvements over the well-established baselines that optimize predefined surrogate functions (such as KMeans, KMedoid, MaxCover, etc.), as well as learning-based graph clustering baselines.

We also provide a theoretical analysis that justifies new techniques such as RS-GNN for RS (as alternatives to combinatorial surrogate functions) and helps explain our empirical results: We show that these surrogate functions can be arbitrarily poor estimators of the optimal model quality by constructing natural learning tasks for which there exists a significant gap between the optimum solution of surrogate functions and the optimal model accuracy. We do this by establishing a new impossibility result for RS, that there does not exist a polynomial-time RS algorithm with an approximation factor better than  $\omega(n^{-1/\text{poly} \log \log n})$ , unless the Exponential Time Hypothesis (ETH) fails. The approximation is with respect to the optimal model accuracy.

Our two main contributions include: 1) Developing RS-GNN for selecting representatives from attributed graphs and showing its merit for datasets with natural and/or similarity graphs (to the best of our knowledge, this is the first work dedicated specifically to this problem), and 2) Providing a hardness result establishing that, under a standard computational-complexity assumption, RS is hard to approximate in polynomial time within any reasonable factor (to the best of our knowledge, this is the first subconstant hardness result for this variant of the RS problem).

## 2 Related Work

The existing works from the literature that are related to our paper can be grouped as follows.

**Representative selection for feature-based data:** Representative selection and feature selection are two sides of the same coin when it comes to compressing or summarizing datasets. Both have been studied extensively via *filter* and *wrapper* methods: evaluation based on final task performance or on some proxy metric of the subset. Examples of such metrics use correlation, redundancy, coverage (or more general submodular functions), or distance of selected entities among each other [43, 51, 8, 5] as well as their mutual information or correlation with the prediction label [22, 50]. While these methods tackle diversity of the sample set [1, 36, 67, 6], there has been extensive attention in the past few years on taking fairness constraints into account as well [41, 54, 42, 58, 4]. Beside random sampling, stratified and quota sampling have been other methods to match the population distribution.

**Active learning:** In active learning [56, 20] we have an unlabeled set of data points which we can request to label. Since labeling is an expensive task, we usually have a limited budget, say, we can label up to  $k$  data points, which are then used to predict the labels of all data points. The goal is to select the set of data points to label in such a way as to maximize the accuracy of the final model. In theory these data points can be chosen one by one: Pick one data point, label it, update the model, and repeat. However, in practice, retraining the model is time-consuming, hence the model is retrained occasionally or only once [33, 29, 12, 19, 3]. In this context, the RS problem considered here can be seen as one-shot active learning. In fact, our hardness result directly applies to active learning as well.

**Graph pooling/clustering:** Graph pooling aims to distill the hierarchical nature of (attributed) graphs via iterative coarsening operations. Coarsening compresses nodes of the graph into “super-nodes,” which are used to aggregate information. Coarsening can be done either through link prediction [65], node clustering [68, 14, 7, 60], or edge sparsification [63, 26, 44]. The RS problem considered here can be seen as a way of pooling information in the graph to the set of selected representatives.

## 3 Notation & Problem Definition

We use bold lowercase letters to denote vectors and bold uppercase letters to denote matrices. Let  $x_i$  represent the  $i^{\text{th}}$  element of  $\mathbf{x}$  and  $M_i$  represent the  $i^{\text{th}}$  row of  $M$ . For a function  $f : A \mapsto B$  and a subset  $A' \subseteq A$ , we use  $f|_{A'}$  to denote the restriction of the domain of  $f$  to  $A'$ . We denote an attributed graph as  $\mathcal{G} = \{\mathcal{V}, \mathbf{A}, \mathbf{X}\}$  where  $\mathcal{V} = \{v_1, \dots, v_m\}$  represents the set of nodes,  $\mathbf{A} \in \mathbb{R}^{m \times m}$  represents the adjacency matrix, and  $\mathbf{X} \in \mathbb{R}^{m \times n}$  represents the matrix of node features ( $m$  nodes and  $n$  features). When nodes have class labels, we use  $c$  to represent the number of classes.

We define the general representative selection problem as follows:

**Definition 3.1 (RS).** Let  $\mathcal{V}$  be a set of data points with additional “context”  $\mathcal{C}$  providing all the observed information about them (e.g., their features). Given  $\mathcal{V}, \mathcal{C}$ , a number  $0 < k \leq |\mathcal{V}|$ , and a

utility function  $u : 2^{\mathcal{V}} \mapsto \mathbb{R}$ , select a subset  $\mathcal{S} \subseteq \mathcal{V}$  of  $k$  representatives to maximize the utility  $u(\mathcal{S})$  ( $\mathcal{V}$  is implicit in the definition of  $u$ , hence RS).

Typically,  $\mathcal{C} = \{\mathbf{X}\}$  where  $\mathbf{X}_i$  corresponds to features of the  $i^{\text{th}}$  data point  $v_i$ . In the case of attributed graphs,  $\mathcal{C} = \{\mathbf{X}, \mathbf{A}\}$ .

In this work, we focus on a concrete learning problem (Representative Search for Learning, or RSL) as a special case of the general formulation above: We get to see the labels of the selected representatives, based on which we aim to train a classifier of highest *normalized accuracy* on the entire dataset. Our algorithms, however, apply to the general case of RS.

**Definition 3.2** (RSL). Let  $\mathcal{V}$  be a set of data points with labels  $y : \mathcal{V} \mapsto \{1, \dots, c\}$ , which is a function of their *observed* and *latent* information. Let  $\mathcal{C}$  denote the “context” (all observed information), while the latent information is hidden from us. Given  $\mathcal{V}, \mathcal{C}$ , and a number  $0 < k \leq |\mathcal{V}|$ , we select a subset  $\mathcal{S}$  of  $k$  representatives from  $\mathcal{V}$  and train a classifier  $\phi : \mathcal{V} \mapsto \{1, \dots, c\}$  based on  $\mathcal{C}$  and  $y|_{\mathcal{S}}$ . Our goal is to maximize the *normalized accuracy* of  $\phi$ .

## 4 Theoretical Findings: Hardness Results for RS

Before presenting our method for selecting representatives from attributed graphs, we describe a theoretical finding that explains why the common practice of hand designing and optimizing surrogate functions may not be a good approach for RSL (and hence RS in general).

In Definition 3.2, let  $u(\mathcal{S}) = \overline{\text{Acc}}(\phi(\mathcal{S}))$  represent the normalized accuracy of the classifier  $\phi$  when trained on a subset  $\mathcal{S}$  of data points, and  $\mathcal{S}^* = \arg \max_{\mathcal{S}} u(\mathcal{S})$  be the optimal set of representatives. Ideally, one would optimize  $u(\mathcal{S})$  and find  $\mathcal{S}^*$ . This may, however, be impossible without a-priori having access to the labels for all data points. Alternatively, most existing works on RSL (and RS in general) focus on defining an intuitive surrogate function  $\Omega$  and find a solution  $\mathcal{S}^\Omega$  by optimizing  $\Omega(\mathcal{S})$  in the hope that  $u(\mathcal{S}^\Omega)$  is a good approximator for  $u(\mathcal{S}^*)$ . In this section, we establish an inapproximability result demonstrating that  $u(\mathcal{S}^\Omega)$  may not be a good estimator of  $u(\mathcal{S}^*)$  for any polynomial-time-computable surrogate function  $\Omega$ . We do this by showing that there are simple and naturally defined learning tasks for which there exists a significant gap between  $u(\mathcal{S}^\Omega)$  and  $u(\mathcal{S}^*)$ .

We start by studying the computational hardness of RSL as an end-to-end task, from which the aforementioned claims follow. To show the hardness of RSL, we focus on a binary classification setting where we measure the accuracy by normalized accuracy formulated as  $\overline{\text{Acc}} = 2(\text{accuracy} - 1/2)$ . We say an RS algorithm  $\mathcal{A}$  (e.g., optimizing a surrogate function) approximates the optimal solution with an approximation factor  $\alpha$  if we can establish that  $u(\mathcal{S}^{\mathcal{A}})$  is within a factor  $\alpha$  of the optimal solution  $u(\mathcal{S}^*)$  for any learning problem, where  $\mathcal{S}^{\mathcal{A}}$  is the solution of the RS algorithm.

We show that, under the Exponential-Time Hypothesis (ETH) assumption<sup>1</sup>, there is no polynomial-time RS algorithm with an approximation factor better than  $\omega(n^{-1/\text{poly} \log \log n})$ . Note that  $\omega(n^{-1/\text{poly} \log \log n})$  is almost polynomial, ruling out the existence of any constant approximation or even poly-logarithmic approximation. In other words, we show that there is a learning problem, for which the gap between  $u(\mathcal{S}^{\mathcal{A}})$  and  $u(\mathcal{S}^*)$  for any polynomial-time RS algorithm  $\mathcal{A}$  is at least  $\omega(n^{-1/\text{poly} \log \log n})$ , unless ETH fails. A similar approximation gap exists between the best polynomial-time and best exponential-time algorithm. Note that the best solution may not give 100% accuracy, nor does it necessarily match the accuracy obtained by using all the labels (since we can only use  $k$ ). We prove this by showing a hardness result for the following learning problem, which is a special case of RSL (hence, of RS).

**Definition 4.1** (Fit-or-Not (FoN) Learning Problem). We have  $m$  data points and  $n$  binary features. Each feature is associated with one of two types: red or blue. The types are generated independently and uniformly at random, they are consistent across data points, and are hidden from the algorithm. Each data point has value 1 for two features and 0 for the rest. The label of a data point is 1 if the type of its features of value 1 are the same, and the label is 0 otherwise. The goal is to maximize test set normalized AUC given labels only on selected data points.

The FoN problem can be naturally framed as RSL by defining the four components from Definition 3.2 as follows: let  $\mathcal{V}$  be the set of  $m$  data points,  $\mathcal{C}$  be a mapping of data points to their  $n$  binary features

<sup>1</sup>A widely-believed assumption (e.g., see [2, 10, 11, 16, 15, 21, 35, 37, 45, 46, 61]) in the domain of parameterized complexity which states that 3-SAT cannot be solved in subexponential time in the worst case.

(or alternatively to the two non-zero entries),  $k$  be the budget for selecting representatives, and let the labels  $y$  be as defined above (where the latent information consists of the types of the  $n$  features). Note that the FoN problem has a simple definition, and hence shows that RS is hard in a very broad form. Moreover, due to the structure of the problem, it is easy to construct an attributed graph for this problem by adding an edge between every two data points sharing a feature of value 1.

The next theorem is the main result of this section.

**Theorem 4.2.** *There is no polynomial-time representative selection algorithm for FoN with an approximation factor better than  $\omega(n^{-1/\text{poly log log } n})$ , unless the exponential-time hypothesis fails.*

*Proof Sketch.* We defer the proof to the Appendix and provide a sketch here. The proof goes by reducing the densest  $k$ -subgraph problem to the FoN problem. In the densest  $k$ -subgraph problem, the goal is to find a subgraph with  $k$  vertices and the maximum number of edges for an unweighted graph. We say an algorithm is an  $\alpha$ -approximation algorithm for the densest  $k$ -subgraph problem if it returns a subgraph with  $k$  vertices where the number of edges is at least  $\alpha$  times that of the densest  $k$ -subgraph. It is known that there is no  $\omega(n^{-1/\text{poly log log } n})$ -approximation polynomial-time algorithm for the densest  $k$ -subgraph problem unless ETH fails [46].

We show how to transform an input of the densest  $k$ -subgraph problem to an input to the FoN problem, and then show how to transform an approximate solution for the FoN problem to an approximate solution for the densest  $k$ -subgraph problem while only increasing the approximation factor by a constant. Therefore an  $\omega(n^{-1/\text{poly log log } n})$ -approximation polynomial-time algorithm for the FoN implies an  $\omega(n^{-1/\text{poly log log } n})$ -approximation polynomial-time algorithm for the densest  $k$ -subgraph problem, which does not exist unless ETH fails.  $\square$

To the best of our knowledge, this is the first subconstant hardness result for RS. Our subconstant hardness result is of particular importance because several previous works have chosen to optimize *surrogate functions*—these can be approximated well in theory—instead of the actual model accuracy. For instance, they consider a submodular surrogate function which can be approximated within a factor  $1 - 1/e$  in polynomial time [28, 64, 48, 17, 23]. Our hardness result implies the following.

**Corollary 4.3.** *In the worst case, there is a significant gap of  $\omega(n^{-1/\text{poly log log } n})$  between  $u(\mathcal{S}^*)$  and the solution of any polynomial-time approximable surrogate function that estimates  $u(\mathcal{S}^*)$ .*

The corollary follows because these surrogate functions can be optimized or approximated accurately in polynomial time, but Theorem 4.2 shows that even for simple learning problems, approximating the accuracy is not possible in polynomial time (assuming the ETH); therefore, there are certain instances of the problem where optimizing for the surrogate functions does not optimize for the learning accuracy within the given approximation factor.

While the above analysis shows a worst-case hardness result, we hypothesize that the gap for different real-world datasets is on a spectrum and that representation learning-based approaches can help reduce the gap by exploiting the structure of the data through jointly optimizing the RS objective and a representation learning objective. We will next develop such an approach for selecting representatives from attributed graphs and present empirical results which corroborate this hypothesis.

## 5 RS-GNN: A Representation Learning-based Model for RS

We develop **RS-GNN**, a representation learning-based approach for **RS** via **GNNs**. When a graph structure is available in the context  $\mathcal{C}$  (cf. Definition 3.1), our GNN uses the available structure. Otherwise, we create a similarity graph of the input node features and feed that structure to our model. We begin with describing two main components used by our model before specifying it completely.

### 5.1 Preliminaries

**Graph Neural Networks (GNNs):** GNNs encode graph-structured data in continuous space [13]. Graph convolutional networks (GCNs) [39] are a powerful variant of GNNs. Let  $\mathcal{G} = \{\mathcal{V}, \mathbf{A}, \mathbf{X}\}$  be an attributed graph,  $\hat{\mathbf{A}} = \mathbf{A} + \mathbf{I}$  be the adjacency matrix of  $\mathcal{G}$  with self-loops included, and  $\mathbf{D}$  be the degree matrix of  $\hat{\mathbf{A}}$ , where  $D_{ii} = \sum_j \hat{A}_{ij}$  and  $D_{ij} = 0$  for  $i \neq j$ . The  $l^{\text{th}}$  layer

of an L-layer GCN model with parameters  $\Theta = \{\mathbf{W}^{(1)}, \dots, \mathbf{W}^{(L)}\}$  can be defined as  $\mathbf{H}^{(l)} = \sigma(\mathbf{D}^{-\frac{1}{2}} \hat{\mathbf{A}} \mathbf{D}^{-\frac{1}{2}} \mathbf{H}^{(l-1)} \mathbf{W}^{(l)})$ , where  $\mathbf{H}^{(l)}$  represents node embeddings in the  $l^{\text{th}}$  layer ( $\mathbf{H}^{(0)} = \mathbf{X}$ ),  $\mathbf{W}^{(l)}$  is a weight matrix, and  $\sigma$  is an activation function. In the rest of the paper, we use  $\text{GCN}(\mathcal{G}; \Theta)$  to show the application of a GCN function with parameters  $\Theta$  on a graph  $\mathcal{G}$ .

**Deep Graph Infomax (DGI):** DGI [62] is an unsupervised representation-learning approach for attributed graphs. Given an attributed graph  $\mathcal{G}$ , in each iteration DGI creates a corrupted graph  $\mathcal{G}'$  from  $\mathcal{G}$ . Then, it computes node embeddings  $\mathbf{H}$  and  $\mathbf{H}'$  for the two graphs by applying a GNN model on them. Then, a summary vector  $s$  is computed from the node embeddings  $\mathbf{H}$ . Finally, a discriminator is simultaneously trained to separate the node embeddings of the original graph (i.e.,  $\mathbf{H}$ ) from those of the corrupted graph (i.e.,  $\mathbf{H}'$ ) based on the summary vector  $s$ . We describe the details of each step in Section 5.4 when we define our final model.

## 5.2 Representative Selection via GNNs

An attributed graph  $\mathcal{G} = \{\mathcal{V}, \mathbf{A}, \mathbf{X}\}$  has two modalities, the node features  $\mathbf{X}$  and the graph structure  $\mathbf{A}$ . To be able to exploit both modalities in selecting good representatives, we employ a function EMB that combines the two modalities into a single embedding matrix of the graph. Concretely,  $\text{EMB}(\mathcal{G}) = \mathbf{H}$ , where  $\mathbf{H} \in \mathbb{R}^{m \times d}$  and  $d$  represents the embedding dimension. We also employ a differentiable function SEL that receives  $\mathbf{H}$  as input and selects  $k$  nodes as representatives. That is,  $\text{SEL}(\mathbf{H}) = \mathcal{S}$ . The two functions are optimized in a multi-task setting with the loss function

$$\mathcal{L} = \mathcal{L}_{\text{EMB}} + \lambda \mathcal{L}_{\text{SEL}}, \quad (1)$$

where  $\mathcal{L}_{\text{EMB}}$  encourages learning informative node embeddings and  $\mathcal{L}_{\text{SEL}}$  encourages selecting good representatives. One can create different RS models with different choices of EMB, SEL,  $\mathcal{L}_{\text{EMB}}$  and  $\mathcal{L}_{\text{SEL}}$ . GNNs have prove effective in learning node embeddings, so we use GNNs as our embedding function EMB. For  $\mathcal{L}_{\text{EMB}}$ , we use the DGI objective which has shown to provide high-quality embeddings in unsupervised settings. For SEL, we consider a representative embedding matrix  $\mathbf{R} \in \mathbb{R}^{k \times d}$  with learnable parameters where  $\mathbf{R}$  is initialized randomly and  $\mathbf{R}_j$  represents the embedding for the  $j^{\text{th}}$  representative. We let

$$\mathcal{L}_{\text{SEL}} = \sum_i \min_j (\text{Dist}(\mathbf{H}_i, \mathbf{R}_j)), \quad (2)$$

where  $\text{Dist}(\mathbf{H}_i, \mathbf{R}_j)$  is the distance between the  $i^{\text{th}}$  node’s embedding  $\mathbf{H}_i$  and the  $j^{\text{th}}$  representative’s embedding  $\mathbf{R}_j$ . We use Euclidean distance as the distance function. Having the representative embedding matrix  $\mathbf{R}$ , we select the representative corresponding to each  $\mathbf{R}_j$  by finding the closest node embedding from  $\mathbf{H}$  to  $\mathbf{R}_j$ , i.e.,  $\text{argmin}_i (\text{Dist}(\mathbf{H}_i, \mathbf{R}_j))$ .

Observe that with the loss function of equation 1, the model can trivially reduce  $\mathcal{L}_{\text{SEL}}$  by making the values in  $\mathbf{H}$  arbitrarily small. That is because multiplying  $\mathbf{H}$  by a small constant may not change  $\mathcal{L}_{\text{EMB}}$  substantially, but it can make the distances between the nodes arbitrarily small, resulting in a low value for  $\mathcal{L}_{\text{SEL}}$  even for a random representative embedding matrix  $\mathbf{R}$ . In the next subsection we describe a normalization scheme, *CenterNorm*, that is applied to  $\mathbf{H}$  before  $\mathbf{H}$  is used in equation 2, which helps avoid this problem.

## 5.3 CenterNorm

As we show in the Appendix, using the DGI loss function results in corrupted node embeddings that form a dense cluster in some part of the embedding space, and node embeddings (from the actual graph) that arrange themselves in subclusters around (and outside) this dense cluster of negative examples. Based on the this observation, we propose an  $\ell_2$  normalization of the node embeddings in  $\mathbf{H}$  with respect to the center of the node embeddings:

$$\boldsymbol{\mu} = \frac{1}{n} \sum_i \mathbf{H}_i, \quad \boldsymbol{\zeta} = \|\mathbf{H} - \boldsymbol{\mu}\|, \quad \tilde{\mathbf{H}} = (\mathbf{H} - \boldsymbol{\mu})/\boldsymbol{\zeta}, \quad (3)$$

where  $\boldsymbol{\mu}$  is the center of the embeddings  $\mathbf{H}$ ,  $\boldsymbol{\zeta}$  is the  $\ell_2$  norms of the nodes with respect to the center, and  $\tilde{\mathbf{H}}$  represents the normalized embeddings. With CenterNorm, the model can no longer decrease  $\mathcal{L}_{\text{SEL}}$  simply by making the values  $\mathbf{H}$  smaller. Note that since the embedding clusters in  $\mathbf{H}$  are at a large angle from each other (cf. Appendix),  $\ell_2$  normalization has a low chance of collapsing two clusters. Furthermore,  $\ell_2$  normalization helps bring the nodes within one cluster closer to each other, which helps in identifying clusters and selecting representatives.

#### 5.4 The Final Model: RS-GNN

The full RS-GNN model is described in Algorithm 1. The input is an attributed graph  $\mathcal{G} = (\mathcal{V}, \mathbf{A}, \mathbf{X})$  and a number  $k$  corresponding to the number of representative nodes that must be selected from the graph. The model initializes  $\mathbf{R}$  (the representative embeddings),  $\Theta$  (the GCN parameters), and  $U$  (the parameters for the DGI discriminator). Lines 3 to 7 compute node embeddings  $\mathbf{H}$  using a GCN model and compute a DGI loss as  $\mathcal{L}_{\text{EMB}}$ . Here,  $\text{bilinear}(\mathbf{H}, \mathbf{s}; U) = \text{sigmoid}(\mathbf{H}^T U \mathbf{s})$  where  $\mathbf{H}^T$  indicates the transpose of  $\mathbf{H}$ . Lines 8 and 9 apply CenterNorm. Lines 10 to 12 compute  $\mathcal{L}_{\text{SEL}}$  based on equation 2 and then  $\mathcal{L}$  based on equation 1 and update the parameters accordingly.

---

#### Algorithm 1 The training procedure of RS-GNN.

---

**Input:**  $\mathcal{G} = (\mathcal{V}, \mathbf{A}, \mathbf{X}), k$

- 1: Initialize  $\mathbf{R}, \Theta$ , and  $U$
- 2: **for** epoch=1 **to** #epochs **do**
- 3:    $\mathcal{G}' = (\mathcal{V}, \mathbf{A}, \text{shuffle}(\mathbf{X}))$
- 4:    $\mathbf{H} = \text{GCN}(\mathcal{G}; \Theta)$ ,  $\mathbf{H}' = \text{GCN}(\mathcal{G}'; \Theta)$
- 5:    $\mathbf{s} = \text{sigmoid}(\frac{1}{n} \sum_i \mathbf{H}_i)$
- 6:    $\mathbf{p} = \text{bilinear}(\mathbf{H}, \mathbf{s}; U)$ ,  $\mathbf{p}' = \text{bilinear}(\mathbf{H}', \mathbf{s}; U)$
- 7:    $\mathcal{L}_{\text{EMB}} = -\sum_i (\log(\mathbf{p}_i) + \log(1 - \mathbf{p}'_i))$
- 8:    $\boldsymbol{\mu} = \frac{1}{n} \sum_i \mathbf{H}_i$ ,  $\zeta = \|\mathbf{H} - \boldsymbol{\mu}\|$
- 9:    $\tilde{\mathbf{H}} = \text{CenterNorm}(\mathbf{H}) = (\mathbf{H} - \boldsymbol{\mu})/\zeta$
- 10:    $\mathcal{L}_{\text{SEL}} = \sum_i \min_j \text{Dist}(\tilde{\mathbf{H}}_i, \mathbf{R}_j)$
- 11:    $\mathcal{L} = \mathcal{L}_{\text{EMB}} + \lambda \mathcal{L}_{\text{SEL}}$
- 12:   Compute gradients based on  $\mathcal{L}$  and upd. parameters.
- 13: Let  $\hat{\mathbf{R}}$  and  $\hat{\mathbf{H}}$  be the representative and normalized node embeddings with minimum  $\mathcal{L}$  during training.
- 14: **for** j=1 **to** k **do**
- 15:   The  $j^{\text{th}}$  representative =  $\text{argmin}_i \text{Dist}(\hat{\mathbf{H}}_i, \hat{\mathbf{R}}_j)$

---

During training, we keep track of the epoch with minimum joint loss  $\mathcal{L}$ . Let  $\hat{\mathbf{R}}$  and  $\hat{\mathbf{H}}$  be the corresponding representative and normalized node embeddings in the best epoch. We select the  $j^{\text{th}}$  representative to be the node whose normalized embedding is closest to the  $j^{\text{th}}$  representative embedding. Lines 13 to 15 select the representatives based on  $\hat{\mathbf{R}}$  and  $\hat{\mathbf{H}}$ .

## 6 Empirical Results

We describe our baselines, datasets, and metrics, and defer implementation details to the Appendix<sup>2</sup>.

**Baselines:** We compare against a representative set of baselines outlined as follows.

- *Random:* Selects  $k$  nodes uniformly at random.
- *Popular:* Selects the  $k$  nodes with the maximum degree from the graph.
- *Surrogate functions on node features:* We test a representative set of surrogate functions including KMedoid, KMeans, Farthest First Search (FFS) and (Greedy) MaxCover. For KMedoid and KMeans, we run the algorithm to create  $k$  clusters. For KMedoid, we use the medoids as the representatives. For KMeans, we select the closest node to each center as a representative. For FFS and MaxCover, we select representatives sequentially. In FFS [66], the next representative is the node farthest away (by Euclidean distance) from the closest representative in the current set. In MaxCover [32], the next representative is the node that increases the coverage of the non-selected nodes the most. For MaxCover, we experiment with RBF kernel and cosine similarities; we use MC (RBF) and MC (cos) to refer to the two versions respectively. The sequential nature of FFS and MC makes them less amenable to parallelization over GPUs/TPUs.
- *Surrogate functions on node embeddings:* We use similar functions as above but apply them on DGI node embeddings as opposed to on the initial node features. Note that when we run these baselines using DGI embeddings as context, their selections are informed by both node features and the graph structure.
- *Graph clustering:* We compare against two current state-of-the-art models for graph clustering, namely MinCut [7] and DMoN [60]. For both models, we create  $k$  clusters, use the (hard) cluster assignments to compute cluster centers, and select the closest point to each cluster center as a representative.

**Datasets:** We use eight established benchmarks in the GNN literature: three widely-used citation networks namely Cora, CiteSeer, and Pubmed [55, 34], a citation network dataset named OGBN-Arxiv [34] which is orders of magnitude larger than the previous three, two datasets from Amazon products corresponding to the Photos and PC categories [57], and two datasets from Microsoft Academic corresponding to the CS and physics authors [57]. The Appendix offers a more detailed

<sup>2</sup>Code: [https://github.com/google-research/google-research/tree/master/rs\\_gnn](https://github.com/google-research/google-research/tree/master/rs_gnn)

Table 1: For each dataset, each algorithm selects  $2c$  representatives. Then, we train a GCN model on the labels of the selected representatives. The reported metric is the test accuracy of the GCN models. Bold numbers indicate statistically significant winner(s) following a t-test (p-value=0.05). OOM indicates out of memory. The color-codes and symbols represent  $\clubsuit$  surrogate functions on features,  $\spadesuit$  surrogate functions on embeddings, and  $\heartsuit$  attributed graph clustering approaches.

Selector	Context	Cora	CiteSeer	Pubmed	Photos	PC	CS	Physics	Arxiv	Avg.
Random	—	49.1 $\pm$ 6.9	33.1 $\pm$ 8.3	52.0 $\pm$ 8.1	70.2 $\pm$ 6.4	65.4 $\pm$ 6.1	72.9 $\pm$ 5.0	73.6 $\pm$ 6.8	49.0 $\pm$ 1.4	58.2
Popular	A	59.2 $\pm$ 1.3	35.5 $\pm$ 0.8	63.3 $\pm$ 0.3	34.9 $\pm$ 0.5	49.9 $\pm$ 2.1	73.1 $\pm$ 1.1	50.5 $\pm$ 0.0	31.3 $\pm$ 0.8	49.7
$\clubsuit$ KMedoid	X	53.7 $\pm$ 5.4	40.3 $\pm$ 2.8	53.2 $\pm$ 1.0	65.8 $\pm$ 1.2	66.9 $\pm$ 1.8	51.8 $\pm$ 1.0	66.6 $\pm$ 1.6	43.9 $\pm$ 1.5	55.3
$\clubsuit$ KMeans	X	32.5 $\pm$ 5.8	35.4 $\pm$ 1.2	50.6 $\pm$ 0.5	72.5 $\pm$ 0.9	70.9 $\pm$ 1.0	66.5 $\pm$ 0.5	73.0 $\pm$ 1.4	48.4 $\pm$ 0.5	56.2
$\clubsuit$ FFS	X	48.5 $\pm$ 8.0	39.3 $\pm$ 6.8	43.1 $\pm$ 4.9	80.0 $\pm$ 5.0	71.5 $\pm$ 3.4	54.6 $\pm$ 2.2	76.6 $\pm$ 2.8	45.2 $\pm$ 0.8	57.3
$\clubsuit$ MC (RBF)	X	45.5 $\pm$ 2.7	25.8 $\pm$ 3.7	53.0 $\pm$ 0.2	78.4 $\pm$ 1.2	65.5 $\pm$ 0.9	66.4 $\pm$ 1.2	58.1 $\pm$ 0.3	51.4 $\pm$ 0.6	55.5
$\clubsuit$ MC (cos)	X	49.7 $\pm$ 9.5	50.2 $\pm$ 3.1	66.6 $\pm$ 0.5	77.2 $\pm$ 1.0	72.4 $\pm$ 0.8	79.3 $\pm$ 0.8	88.3 $\pm$ 1.0	50.0 $\pm$ 0.5	66.7
$\spadesuit$ KMedoid	DGI	48.4 $\pm$ 4.4	34.1 $\pm$ 1.9	60.9 $\pm$ 5.3	81.5 $\pm$ 2.6	69.8 $\pm$ 3.4	82.5 $\pm$ 2.9	81.2 $\pm$ 7.0	OOM	—
$\spadesuit$ KMeans	DGI	62.6 $\pm$ 9.3	42.7 $\pm$ 6.3	60.5 $\pm$ 6.3	83.6 $\pm$ 2.9	<b>74.8</b> $\pm$ 2.7	86.9 $\pm$ 1.8	<b>90.6</b> $\pm$ 2.4	51.2 $\pm$ 1.0	69.1
$\spadesuit$ FFS	DGI	62.6 $\pm$ 4.5	50.4 $\pm$ 5.7	46.7 $\pm$ 7.2	73.4 $\pm$ 5.7	63.5 $\pm$ 6.4	84.8 $\pm$ 5.3	83.4 $\pm$ 5.0	48.6 $\pm$ 2.2	64.2
$\spadesuit$ MC (RBF)	DGI	66.3 $\pm$ 2.6	35.3 $\pm$ 4.5	54.9 $\pm$ 5.3	37.4 $\pm$ 3.7	50.7 $\pm$ 2.5	65.2 $\pm$ 1.2	59.8 $\pm$ 5.1	41.2 $\pm$ 1.6	51.4
$\spadesuit$ MC (cos)	DGI	67.3 $\pm$ 5.2	49.0 $\pm$ 4.1	<b>67.3</b> $\pm$ 1.1	84.4 $\pm$ 1.0	<b>74.0</b> $\pm$ 3.7	87.3 $\pm$ 1.4	81.3 $\pm$ 3.4	47.6 $\pm$ 1.6	70.0
$\heartsuit$ MinCUT	X, A	51.9 $\pm$ 7.5	37.3 $\pm$ 8.0	59.5 $\pm$ 6.1	14.4 $\pm$ 7.5	18.3 $\pm$ 8.7	85.5 $\pm$ 1.4	86.0 $\pm$ 3.3	32.4 $\pm$ 5.2	48.2
$\heartsuit$ DMoN	X, A	58.0 $\pm$ 7.1	40.5 $\pm$ 7.4	55.3 $\pm$ 7.5	78.6 $\pm$ 9.2	70.3 $\pm$ 3.3	84.3 $\pm$ 1.4	85.9 $\pm$ 3.8	<b>52.5</b> $\pm$ 1.9	65.7
RS-GNN	X, A	<b>71.8</b> $\pm$ 3.0	<b>54.7</b> $\pm$ 3.9	65.8 $\pm$ 3.0	<b>86.3</b> $\pm$ 1.4	<b>74.3</b> $\pm$ 1.7	<b>89.3</b> $\pm$ 0.8	<b>90.0</b> $\pm$ 2.6	<b>52.6</b> $\pm$ 1.2	<b>73.1</b>

description of datasets and their statistics. Our datasets have a wide range in terms of the number of nodes (from 2K to 170K), edges (from 4.5K to 1.1M), features (from 100 to 8.5K) and classes (from 3 to 40). For our experiments on non-graph data, we use the same datasets as above but hide the original graph structure from the models.

**Measures:** For each dataset, once a set  $\mathcal{S} \subseteq \mathcal{V}$  of nodes are selected as representatives by an algorithm, we measure the quality of the selected representatives using the following transductive semi-supervised node-classification problem. We train a GCN model on the dataset where the parameters of the GCN are learned only based on the labels of the nodes in  $\mathcal{S}$ . Note that this GCN is completely independent of the internal GCN model used in RS-GNN. We randomly split the remaining nodes into validation and test sets. The validation set is used for early stopping. The classification accuracy on the test set is used as the metric for measuring the quality of the selected representatives. Considering a validation set for early stopping reduces the chances of overfitting for the classifier and makes the reported test accuracy mainly a function of the quality of the selected representatives. Details of the GCN classifier are provided in the Appendix.

While our model is developed mainly for RS, it can also be used for graph clustering by assigning each node to its closest representative. To measure the quality of clusters produced by our model, we set  $k$  to be equal to  $c$  (i.e., the number of classes) for each dataset, and then compute the normalized mutual information (NMI) score between the clusters and the node labels.

## 6.1 Results: RS for Attributed Graphs

The results of our model and the baselines are presented in Table 1. For the results in this table, we set  $k$  for each dataset to be  $2c$ , where  $c$  represents the number of classes. We found this to be a small enough number for a meaningful comparison of the quality of the selected representatives<sup>3</sup>, and high enough for the classification GCN model to learn appropriate functions of the data. Since  $c$  is different for each dataset, making  $k$  a function of  $c$  also provides the opportunity to compare performance not only in terms of variation in the datasets, but also in terms of variation in the number of selected representatives.

We start by analyzing the baseline results. The random baseline is already a strong baseline outperforming some of the other models on some datasets. However, it comes with a high standard deviation which makes it unreliable. The *popular* baseline provides a much smaller standard deviation and

<sup>3</sup>Note that if  $k \approx n$ , all models may perform equally well.

Table 2: Classification accuracies when a graph structure is not provided as input. Selecting  $5c$  representatives. Bold numbers indicate statistically significant winner(s) following a t-test (p-value=0.05).

Selector	Classifier	Context	Cora	CiteSeer	Pubmed	Photos	PC	CS	Physics	Avg.
Random	MLP	X	41.9 $\pm$ 2.9	37.4 $\pm$ 4.0	51.9 $\pm$ 5.0	57.5 $\pm$ 4.0	55.2 $\pm$ 4.4	76.1 $\pm$ 2.7	76.7 $\pm$ 5.2	56.7
Random	kNN-GCN	X	57.7 $\pm$ 4.1	57.7 $\pm$ 4.5	59.6 $\pm$ 4.6	79.2 $\pm$ 3.4	71.8 $\pm$ 4.4	84.8 $\pm$ 2.2	86.0 $\pm$ 2.9	71.0
KMedoid	MLP	X	39.3 $\pm$ 0.9	33.4 $\pm$ 0.7	46.1 $\pm$ 1.0	40.6 $\pm$ 0.9	47.5 $\pm$ 0.8	62.8 $\pm$ 1.6	67.0 $\pm$ 0.8	48.1
KMedoid	kNN-GCN	X	52.5 $\pm$ 1.4	57.4 $\pm$ 0.8	55.0 $\pm$ 0.7	72.3 $\pm$ 0.6	63.4 $\pm$ 1.8	66.2 $\pm$ 2.9	70.8 $\pm$ 0.3	62.5
KMeans	MLP	X	42.4 $\pm$ 0.9	40.1 $\pm$ 1.1	58.5 $\pm$ 1.3	70.0 $\pm$ 1.0	63.7 $\pm$ 0.8	68.5 $\pm$ 0.7	77.4 $\pm$ 0.3	60.1
KMeans	kNN-GCN	X	56.5 $\pm$ 0.8	55.9 $\pm$ 0.8	<b>72.7</b> $\pm$ 0.3	80.9 $\pm$ 0.6	<b>75.8</b> $\pm$ 0.6	80.0 $\pm$ 0.4	83.7 $\pm$ 0.8	72.2
FFS	MLP	X	39.2 $\pm$ 3.7	44.0 $\pm$ 3.1	43.1 $\pm$ 3.0	60.2 $\pm$ 3.8	55.8 $\pm$ 1.9	56.3 $\pm$ 0.9	77.7 $\pm$ 2.5	53.8
FFS	kNN-GCN	X	56.9 $\pm$ 2.6	62.3 $\pm$ 3.7	48.8 $\pm$ 3.9	80.7 $\pm$ 2.0	<b>74.8</b> $\pm$ 2.5	59.8 $\pm$ 2.5	84.0 $\pm$ 2.1	66.8
MC (cos)	MLP	X	46.5 $\pm$ 2.2	47.5 $\pm$ 2.3	52.1 $\pm$ 0.7	54.0 $\pm$ 2.4	58.2 $\pm$ 1.2	83.0 $\pm$ 0.5	86.8 $\pm$ 0.7	61.2
MC (cos)	kNN-GCN	X	62.0 $\pm$ 1.7	<b>63.0</b> $\pm$ 2.5	59.3 $\pm$ 1.3	79.5 $\pm$ 0.5	<b>75.4</b> $\pm$ 1.1	<b>87.6</b> $\pm$ 0.3	<b>92.8</b> $\pm$ 0.3	74.2
RS-GNN	kNN-GCN	X	<b>64.6</b> $\pm$ 2.4	<b>64.3</b> $\pm$ 2.1	65.1 $\pm$ 3.0	<b>82.2</b> $\pm$ 2.0	<b>75.5</b> $\pm$ 2.1	<b>88.3</b> $\pm$ 1.6	89.9 $\pm$ 1.9	<b>75.7</b>

performs well on some datasets (such as Pubmed), but it is clear from the results that it is not a good heuristic for all benchmarks.

For the surrogate functions KMedoid, KMeans, FFS, and MaxCover, considering the DGI embeddings as opposed to only node features provides a large boost in performance in most cases. This confirms that the node embeddings contain valuable structural information and taking this information into account while selecting representatives is crucial. Among the four baselines, MC (cos) and KMeans perform best. We found FFS to be sensitive to outliers. We also found it difficult to select a set of hyperparameters for MC (RBF) that work well across datasets.

MinCut and DMoN outperform many of the other baselines on several datasets. We found MinCut to produce degenerate solutions for Photos and PC datasets in many runs (assigning all nodes to one cluster), hence performing poorly on them. DMoN, on the other hand, shows consistently good results on our datasets. Both baselines show a rather high variance across different runs.

RS-GNN performs well across all datasets and consistently outperforms (or matches) the baselines (with the exception of Pubmed). It also has a lower variance across different runs which makes it a more reliable model. It achieves 4.4% improvement over the best surrogate function baseline, and 11.3% improvement over the best graph clustering baseline, when averaging across all datasets.

## 6.2 Results: RS Without a Graph Structure

So far, we assumed the availability of a graph structure between the nodes that specifies their connectivity. In several applications, such a graph may not be readily available. For semi-supervised node classification, it has recently been shown that even when a graph structure is not available but the nodes are known to have an underlying relation, one can still leverage GNNs by learning both a graph structure and GNN parameters simultaneously [24]. Such a model has been shown to outperform other approaches that make decisions only based on node features.

We extend the aforementioned results to the RS problem. In particular, we assume we have access *only* to the node features of our datasets, and not to their graph structures. The baselines select representatives only based on the node features. For RS-GNN, we first create a kNN similarity graph between the nodes and then run the model on the node features and the created graph. The kNN graph is computed once and then fixed during training; we leave further experiments with learning the graph structure as future work. Notice that all models have access to the same context.

Once the representatives are selected, we train GCN classifiers on the labels of the selected nodes similar to experiments in Section 6.1. For the baselines, we run our classification GCN in two settings: (1) the only edges in the graph are self-loops, (2) the edges in the graph are those from a kNN similarity graph. We call the classifier in the former setting a multi-layer perceptron (MLP) and the one in the latter setting a kNN-GCN. Since a graph structure is not available for this experiment, we only report results for the top baselines that operate on node features only.

Since without having access to the graph structures there exists less signal in the datasets, we allow each model to select  $5c$  representatives for the experiments in this section. The results are presented



Table 3: Normalized mutual information (NMI) scores between the ground-truth labels of nodes and their cluster assignments. All baselines results are from [60]. Bold numbers indicate the winners.

Selector	Context	Cora	CiteSeer	Pubmed	Photos	PC	CS	Physics	Avg.
KMeans	X	18.5	24.5	19.4	28.8	21.1	35.7	30.6	25.5
SBM	A	36.2	15.3	16.4	59.3	48.4	58.0	45.4	39.9
MinCut	X, A	35.8	25.9	25.4	—	—	64.6	48.3	—
DMoN	X, A	48.8	33.7	<b>29.8</b>	<b>63.3</b>	49.3	69.1	51.9	49.4
RS-GNN	X, A	<b>55.4<math>\pm</math>0.8</b>	<b>41.3<math>\pm</math>1.0</b>	26.1 $\pm$ 3.6	58.3 $\pm$ 1.6	<b>50.1<math>\pm</math>0.9</b>	<b>75.8<math>\pm</math>1.2</b>	<b>56.9<math>\pm</math>3.3</b>	<b>52.0</b>

in Table 2. We initially observe that regardless of the selection strategy, using kNN-GCN as the classifier improves the results. This is consistent with the results of [24]. More importantly, the results show that selecting representatives using RS-GNN performs consistently well on all datasets and provides a boost compared to our baselines on many of the datasets. This confirms that RS-GNN is an effective RS algorithm for datasets where a graph structure is not available but the data points have a hidden underlying structure.

### 6.3 Results: Clustering Performance

The goal of attributed-graph clustering is to cluster the nodes based on similarity of their features and structural properties. While we developed RS-GNN mainly for the RS problem, it can also be used for graph clustering: simply assign each node to its closest representative. To assess the performance of our model (vs other clustering methods) on attributed-graph clustering, we cluster the nodes in each dataset into  $c$  groups (recall that  $c$  is the number of classes) using the nearest representative. Then, we compute the normalized mutual information (NMI) score, an established score for measuring and comparing clustering algorithms, between the cluster assignments and the node labels.

The results are presented in Table 3. There, the SBM baseline works by estimating [53] a constrained Stochastic Block Model [59] with given number of  $k$  clusters, effectively maximizing the modularity [49] of the network. RS-GNN outperforms the baselines on five out of seven datasets. Averaging over all seven datasets, our model achieves 5.3% improvement over the best performing baseline, showing that RS-GNN is also an effective method for attributed-graph clustering.

### 6.4 Visualization

In Figure 1, we use UMAP [47] to visualize the learned embeddings and the selected representatives of RS-GNN for the Cora dataset. The plot for CiteSeer appears in the Appendix. The colors in the plot represent the class to which the node or the representative belongs. It can be observed that the nodes from each class have formed one or more dense clusters. Furthermore, it can be observed that our model has selected a representative from (almost all of) these dense regions of points.

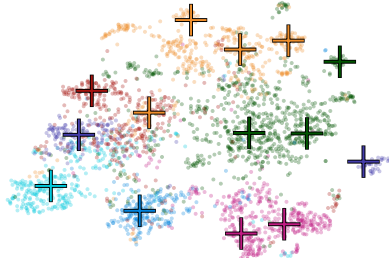


Figure 1: A UMAP visualization of the node embeddings and the selected representatives for Cora. The colors represent the class to which the nodes/representatives belong.

## 7 Conclusion

In this paper, we studied the representative selection (RS) problem theoretically and empirically. We proved new hardness results showing it is impossible to provide a polynomial-time algorithm for RS with an approximation within any reasonable factor, unless the exponential time hypothesis fails. The hardness result explains the significant gap between the accuracy of models trained on optimal representatives and the widely-used surrogate functions for the RS problem, and, in turn, justifies new techniques to solve this problem. In light of this result we proposed RS-GNN to optimize the RS task via graph neural networks, and showed its effectiveness on a suite of different datasets and tasks.

## References

- [1] Zeinab Abbassi, Vahab S. Mirrokni, and Mayur Thakur. Diversity maximization under matroid constraints. In Inderjit S. Dhillon, Yehuda Koren, Rayid Ghani, Ted E. Senator, Paul Bradley, Rajesh Parekh, Jingrui He, Robert L. Grossman, and Ramasamy Uthurusamy, editors, *The 19th ACM SIGKDD International Conference on Knowledge Discovery and Data Mining, KDD 2013, Chicago, IL, USA, August 11-14, 2013*, pages 32–40. ACM, 2013.
- [2] Divesh Aggarwal and Noah Stephens-Davidowitz. (gap/s) eth hardness of svp. In *Proceedings of the 50th Annual ACM SIGACT Symposium on Theory of Computing*, pages 228–238, 2018.
- [3] Kareem Amin, Corinna Cortes, Giulia DeSalvo, and Afshin Rostamizadeh. Understanding the effects of batching in online active learning. In *International Conference on Artificial Intelligence and Statistics*, pages 3482–3492. PMLR, 2020.
- [4] Martin Aumüller, Sariel Har-Peled, Sepideh Mahabadi, Rasmus Pagh, and Francesco Silvestri. Fair near neighbor search via sampling. *SIGMOD Rec.*, 50(1):42–49, 2021.
- [5] MohammadHossein Bateni, Hossein Esfandiari, and Vahab S. Mirrokni. Optimal distributed submodular optimization via sketching. In Yike Guo and Faisal Farooq, editors, *Proceedings of the 24th ACM SIGKDD International Conference on Knowledge Discovery & Data Mining, KDD 2018, London, UK, August 19-23, 2018*, pages 1138–1147. ACM, 2018.
- [6] Aditya Bhaskara, Mehrdad Ghadiri, Vahab S. Mirrokni, and Ola Svensson. Linear relaxations for finding diverse elements in metric spaces. In Daniel D. Lee, Masashi Sugiyama, Ulrike von Luxburg, Isabelle Guyon, and Roman Garnett, editors, *Advances in Neural Information Processing Systems 29: Annual Conference on Neural Information Processing Systems 2016, December 5-10, 2016, Barcelona, Spain*, pages 4098–4106, 2016.
- [7] Filippo Maria Bianchi, Daniele Grattarola, and Cesare Alippi. Spectral clustering with graph neural networks for graph pooling. In *International Conference on Machine Learning*, pages 874–883. PMLR, 2020.
- [8] Verónica Bolón-Canedo, Noelia Sánchez-Marroño, and Amparo Alonso-Betanzos. Recent advances and emerging challenges of feature selection in the context of big data. *Knowl. Based Syst.*, 86:33–45, 2015.
- [9] James Bradbury, Roy Frostig, Peter Hawkins, Matthew James Johnson, Chris Leary, Dougal Maclaurin, George Necula, Adam Paszke, Jake VanderPlas, Skye Wanderman-Milne, and Qiao Zhang. JAX: composable transformations of Python+NumPy programs. 2018.
- [10] Mark Braverman, Young Kun Ko, Aviad Rubinfeld, and Omri Weinstein. Eth hardness for densest-k-subgraph with perfect completeness. In *Proceedings of the Twenty-Eighth Annual ACM-SIAM Symposium on Discrete Algorithms*, pages 1326–1341. SIAM, 2017.
- [11] Mark Braverman, Young Kun Ko, and Omri Weinstein. Approximating the best nash equilibrium in no (log n)-time breaks the exponential time hypothesis. In *Proceedings of the twenty-sixth annual ACM-SIAM symposium on Discrete algorithms*, pages 970–982. SIAM, 2014.
- [12] Shayok Chakraborty, Vineeth Balasubramanian, and Sethuraman Panchanathan. Adaptive batch mode active learning. *IEEE transactions on neural networks and learning systems*, 26(8):1747–1760, 2014.
- [13] Ines Chami, Sami Abu-El-Haija, Bryan Perozzi, Christopher Ré, and Kevin Murphy. Machine learning on graphs: A model and comprehensive taxonomy. *arXiv preprint arXiv:2005.03675*, 2020.
- [14] Haoran Chen, Zhongjing Yu, Qinli Yang, and Junming Shao. Attributed graph clustering with subspace stochastic block model. *Information Sciences*, 535:130–141, 2020.
- [15] Lin Chen, Hossein Esfandiari, Gang Fu, Vahab S Mirrokni, and Qian Yu. Feature cross search via submodular optimization. *arXiv preprint arXiv:2107.02139*, 2021.
- [16] Yijia Chen, Kord Eickmeyer, and Jörg Flum. The exponential time hypothesis and the parameterized clique problem. In *International Symposium on Parameterized and Exact Computation*, pages 13–24. Springer, 2012.
- [17] Yuxin Chen and Andreas Krause. Near-optimal batch mode active learning and adaptive submodular optimization. In *International Conference on Machine Learning*, pages 160–168. PMLR, 2013.

- [18] Richard Church and Charles ReVelle. The maximal covering location problem. In *Papers of the regional science association*, pages 101–118. Springer-Verlag, 1974.
- [19] Gui Citovsky, Giulia DeSalvo, Claudio Gentile, Lazaros Karydas, Anand Rajagopalan, Afshin Rostamizadeh, and Sanjiv Kumar. Batch active learning at scale. *Advances in Neural Information Processing Systems*, 34, 2021.
- [20] David A Cohn, Zoubin Ghahramani, and Michael I Jordan. Active learning with statistical models. *Journal of artificial intelligence research*, 4:129–145, 1996.
- [21] Marek Cygan, Fedor V Fomin, Łukasz Kowalik, Daniel Lokshtanov, Dániel Marx, Marcin Pilipczuk, Michał Pilipczuk, and Saket Saurabh. Lower bounds based on the exponential-time hypothesis. In *Parameterized Algorithms*, pages 467–521. Springer, 2015.
- [22] Chris H. Q. Ding and Hanchuan Peng. Minimum redundancy feature selection from microarray gene expression data. In *2nd IEEE Computer Society Bioinformatics Conference, CSB 2003, Stanford, CA, USA, August 11-14, 2003*, pages 523–529. IEEE Computer Society, 2003.
- [23] Hossein Esfandiari, Amin Karbasi, and Vahab Mirrokni. Adaptivity in adaptive submodularity. In *Conference on Learning Theory*, pages 1823–1846. PMLR, 2021.
- [24] Bahare Fatemi, Layla El Asri, and Seyed Mehran Kazemi. Slaps: Self-supervision improves structure learning for graph neural networks. In *Neural Information Processing Systems (NeurIPS)*, 2021.
- [25] Dan Feldman. *Coresets and Their Applications*. Citeseer, 2010.
- [26] Hongyang Gao and Shuiwang Ji. Graph U-nets. In *ICML*, 2019.
- [27] Jonathan Godwin\*, Thomas Keck\*, Peter Battaglia, Victor Bapst, Thomas Kipf, Yujia Li, Kimberly Stachenfeld, Petar Veličković, and Alvaro Sanchez-Gonzalez. Jraph: A library for graph neural networks in jax. 2020.
- [28] Andrew Guillory. *Active Learning and Submodular Functions*. University of Washington, 2012.
- [29] Yuhong Guo and Dale Schuurmans. Discriminative batch mode active learning. In *NIPS*, pages 593–600. Citeseer, 2007.
- [30] Kaiming He, Xiangyu Zhang, Shaoqing Ren, and Jian Sun. Delving deep into rectifiers: Surpassing human-level performance on imagenet classification. In *Proceedings of the IEEE international conference on computer vision*, pages 1026–1034, 2015.
- [31] Jonathan Heek, Anselm Levskaya, Avital Oliver, Marvin Ritter, Bertrand Rondepierre, Andreas Steiner, and Marc van Zee. Flax: A neural network library and ecosystem for JAX. 2020.
- [32] Dorit S Hochbaum and Anu Pathria. Analysis of the greedy approach in problems of maximum k-coverage. *Naval Research Logistics (NRL)*, 45(6):615–627, 1998.
- [33] Steven CH Hoi, Rong Jin, Jianke Zhu, and Michael R Lyu. Batch mode active learning and its application to medical image classification. In *Proceedings of the 23rd international conference on Machine learning*, pages 417–424, 2006.
- [34] Weihua Hu, Matthias Fey, Marinka Zitnik, Yuxiao Dong, Hongyu Ren, Bowen Liu, Michele Catasta, and Jure Leskovec. Open graph benchmark: Datasets for machine learning on graphs. *arXiv preprint arXiv:2005.00687*, 2020.
- [35] Joey Huchette, Haihao Lu, Hossein Esfandiari, and Vahab Mirrokni. Contextual reserve price optimization in auctions via mixed-integer programming. *arXiv preprint arXiv:2002.08841*, 2020.
- [36] Piotr Indyk, Sepideh Mahabadi, Mohammad Mahdian, and Vahab S. Mirrokni. Composable core-sets for diversity and coverage maximization. In Richard Hull and Martin Grohe, editors, *Proceedings of the 33rd ACM SIGMOD-SIGACT-SIGART Symposium on Principles of Database Systems, PODS’14, Snowbird, UT, USA, June 22-27, 2014*, pages 100–108. ACM, 2014.
- [37] Peter Jonsson, Victor Lagerkvist, Gustav Nordh, and Bruno Zanuttini. Complexity of sat problems, clone theory and the exponential time hypothesis. In *Proceedings of the twenty-fourth annual ACM-SIAM symposium on Discrete algorithms*, pages 1264–1277. SIAM, 2013.
- [38] Krishnateja Killamsetty, Xujiang Zhao, Feng Chen, and Rishabh Iyer. Retrieve: Coreset selection for efficient and robust semi-supervised learning. *Advances in Neural Information Processing Systems*, 34, 2021.

- [39] Thomas N Kipf and Max Welling. Semi-supervised classification with graph convolutional networks. *arXiv preprint arXiv:1609.02907*, 2016.
- [40] Günter Klambauer, Thomas Unterthiner, Andreas Mayr, and Sepp Hochreiter. Self-normalizing neural networks. In *Proceedings of the 31st international conference on neural information processing systems*, pages 972–981, 2017.
- [41] Ziyi Kou, Yang Zhang, Lanyu Shang, and Dong Wang. Faircrowd: Fair human face dataset sampling via batch-level crowdsourcing bias inference. In *2021 IEEE/ACM 29th International Symposium on Quality of Service (IWQOS)*, pages 1–10, 2021.
- [42] Jae-Gil Lee, Yuji Roh, Hwanjun Song, and Steven Euijong Whang. Machine learning robustness, fairness, and their convergence. In Feida Zhu, Beng Chin Ooi, and Chunyan Miao, editors, *KDD '21: The 27th ACM SIGKDD Conference on Knowledge Discovery and Data Mining, Virtual Event, Singapore, August 14-18, 2021*, pages 4046–4047. ACM, 2021.
- [43] J.G. Lee and C.G. Chung. An optimal representative set selection method. *Information and Software Technology*, 42(1):17–25, 2000.
- [44] Junhyun Lee, Inyeop Lee, and Jaewoo Kang. Self-attention graph pooling. In *ICML*, 2019.
- [45] Daniel Lokshtanov, Dániel Marx, Saket Saurabh, et al. Lower bounds based on the exponential time hypothesis. *Bulletin of the EATCS*, pages 41–72, 2011.
- [46] Pasin Manurangsi. Almost-polynomial ratio eth-hardness of approximating densest k-subgraph. In *Proceedings of the 49th Annual ACM SIGACT Symposium on Theory of Computing*, pages 954–961, 2017.
- [47] Leland McInnes, John Healy, and James Melville. Umap: Uniform manifold approximation and projection for dimension reduction. *arXiv preprint arXiv:1802.03426*, 2018.
- [48] Baharan Mirzasoleiman, Jeff Bilmes, and Jure Leskovec. Coresets for data-efficient training of machine learning models. In *International Conference on Machine Learning*, pages 6950–6960. PMLR, 2020.
- [49] Mark EJ Newman. Modularity and community structure in networks. *Proceedings of the national academy of sciences*, 103(23):8577–8582, 2006.
- [50] Jana Novovicová, Petr Somol, Michal Haindl, and Pavel Pudil. Conditional mutual information based feature selection for classification task. In Luis Rueda, Domingo Mery, and Josef Kittler, editors, *Progress in Pattern Recognition, Image Analysis and Applications, 12th Iberoamericann Congress on Pattern Recognition, CIARP 2007, Valparaiso, Chile, November 13-16, 2007, Proceedings*, volume 4756 of *Lecture Notes in Computer Science*, pages 417–426. Springer, 2007.
- [51] Feng Pan, Wei Wang, Anthony K. H. Tung, and Jiong Yang. Finding representative set from massive data. In *Proceedings of the 5th IEEE International Conference on Data Mining (ICDM 2005), 27-30 November 2005, Houston, Texas, USA*, pages 338–345. IEEE Computer Society, 2005.
- [52] Fabian Pedregosa, Gaël Varoquaux, Alexandre Gramfort, Vincent Michel, Bertrand Thirion, Olivier Grisel, Mathieu Blondel, Peter Prettenhofer, Ron Weiss, Vincent Dubourg, et al. Scikit-learn: Machine learning in python. *the Journal of machine Learning research*, 12:2825–2830, 2011.
- [53] Tiago P Peixoto. Efficient monte carlo and greedy heuristic for the inference of stochastic block models. *Physical Review E*, 89(1):012804, 2014.
- [54] Yuji Roh, Kangwook Lee, Steven Euijong Whang, and Changho Suh. Fairbatch: Batch selection for model fairness. In *9th International Conference on Learning Representations, ICLR 2021, Virtual Event, Austria, May 3-7, 2021*. OpenReview.net, 2021.
- [55] Prithviraj Sen, Galileo Namata, Mustafa Bilgic, Lise Getoor, Brian Galligher, and Tina Eliassi-Rad. Collective classification in network data. *AI magazine*, 29(3):93–93, 2008.
- [56] Burr Settles. Active learning literature survey. 2009.
- [57] Oleksandr Shchur, Maximilian Mumme, Aleksandar Bojchevski, and Stephan Günnemann. Pitfalls of graph neural network evaluation. *arXiv preprint arXiv:1811.05868*, 2018.

- [58] Shubhanshu Shekhar, Greg Fields, Mohammad Ghavamzadeh, and Tara Javidi. Adaptive sampling for minimax fair classification. In A. Beygelzimer, Y. Dauphin, P. Liang, and J. Wortman Vaughan, editors, *Advances in Neural Information Processing Systems*, 2021.
- [59] Tom AB Snijders and Krzysztof Nowicki. Estimation and prediction for stochastic blockmodels for graphs with latent block structure. *Journal of classification*, 1997.
- [60] Anton Tsitsulin, John Palowitch, Bryan Perozzi, and Emmanuel Müller. Graph clustering with graph neural networks. *arXiv preprint arXiv:2006.16904*, 2020.
- [61] Virginia Vassilevska Williams. Hardness of easy problems: Basing hardness on popular conjectures such as the strong exponential time hypothesis (invited talk). In *10th International Symposium on Parameterized and Exact Computation (IPEC 2015)*. Schloss Dagstuhl-Leibniz-Zentrum fuer Informatik, 2015.
- [62] Petar Velickovic, William Fedus, William L Hamilton, Pietro Liò, Yoshua Bengio, and R Devon Hjelm. Deep graph infomax. *ICLR*, 2(3):4, 2019.
- [63] Yue Wang, Yongbin Sun, Ziwei Liu, Sanjay E Sarma, Michael M Bronstein, and Justin M Solomon. Dynamic graph CNN for learning on point clouds. *ACM Transactions on Graphics*, 2019.
- [64] Kai Wei, Rishabh Iyer, and Jeff Bilmes. Submodularity in data subset selection and active learning. In *International Conference on Machine Learning*, pages 1954–1963. PMLR, 2015.
- [65] Zhitao Ying, Jiaxuan You, Christopher Morris, Xiang Ren, Will Hamilton, and Jure Leskovec. Hierarchical graph representation learning with differentiable pooling. In *NeurIPS*, 2018.
- [66] Chong You, Chi Li, Daniel Robinson, and Rene Vidal. Self-representation based unsupervised exemplar selection in a union of subspaces. *IEEE Transactions on Pattern Analysis and Machine Intelligence*, 2020.
- [67] Sepehr Abbasi Zadeh, Mehrdad Ghadiri, Vahab S. Mirrokni, and Morteza Zadimoghaddam. Scalable feature selection via distributed diversity maximization. In Satinder P. Singh and Shaul Markovitch, editors, *Proceedings of the Thirty-First AAAI Conference on Artificial Intelligence, February 4-9, 2017, San Francisco, California, USA*, pages 2876–2883. AAAI Press, 2017.
- [68] Xiaotong Zhang, Han Liu, Qimai Li, and Xiao-Ming Wu. Attributed graph clustering via adaptive graph convolution. In *Proceedings of the Twenty-Eighth International Joint Conference on Artificial Intelligence, IJCAI-19*, pages 4327–4333. International Joint Conferences on Artificial Intelligence Organization, 7 2019.

## A More Empirical Results & Analyses

**Selecting more representatives:** In the main text, we presented results for the case where we selected  $2c$  representatives from each dataset, where  $c$  is the number of classes. Here, we present more results for the case where we select  $5c$  representatives from each class. We limit our baselines to the most competitive/informative ones. The results are in Table 4. We can observe that the performance for all models improves when more representatives are selected. We can also observe that the gap between the models shrinks when more representatives are selected (even the random baseline now shows a competitive performance). Nevertheless, RS-GNN shows a similar trend as when we selected  $2c$  representatives and outperforms the baselines when averaged across datasets.

**Visualization:** In the main text, we provided a UMAP visualization of the learned embeddings and the selected representatives for Cora. In Figure 2, we provide a similar visualization for CiteSeer. Similar behaviour as that of Cora can be observed for CiteSeer, where node embeddings form clusters and a representative is selected from each of the dense clusters.

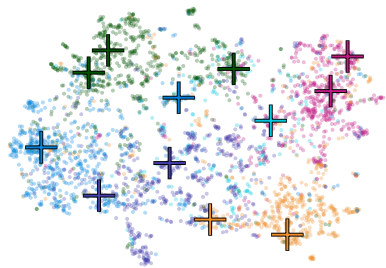


Figure 2: A UMAP visualization of the node embeddings and the selected representatives for CiteSeer. The colors represent the class to which the node or the representative belongs.

Table 4: For each dataset, each algorithm selects  $5c$  representative nodes. Then, we train a GCN model on the labels of the selected representatives. The reported metric is the test accuracy of the GCN models.

Method	Data	Cora	CiteSeer	Pubmed	Photos	PC	CS	Physics	Arxiv	Avg.
Random	A	66.3±4.6	47.3±6.6	62.0±8.3	84.0±3.5	76.8±3.4	83.9±2.3	84.4±5.8	54.6±1.2	69.9
Popular	A	64.1±0.6	43.2±1.4	63.4±0.9	43.9±1.1	54.1±1.4	78.6±0.5	50.5±0.0	42.6±1.4	55.0
KMedoid	X	62.2±1.3	42.1±3.1	60.8±0.3	78.8±0.6	74.4±1.2	63.9±1.7	64.3±0.6	50.6±0.5	62.1
KMeans	X	66.7±1.1	53.8±1.3	71.6±0.5	84.8±1.0	81.4±0.7	76.7±1.0	80.6±0.3	56.8±0.3	71.6
MC (cos)	X	71.3±2.8	59.0±2.8	64.8±0.3	87.5±0.4	78.3±0.7	88.4±0.2	92.4±0.4	56.2±0.5	74.7
KMeans	DGI	74.9±3.1	54.3±4.8	69.3±3.2	89.4±1.3	82.0±1.4	89.2±0.8	92.1±0.7	55.1±1.1	75.8
MC (cos)	DGI	75.8±1.7	59.8±2.5	70.6±2.4	90.0±1.2	82.3±1.1	89.4±0.8	86.1±1.9	55.8±0.7	76.2
MinCUT	X, A	66.8±4.3	48.7±6.6	69.0±4.2	16.7±8.1	16.5±10.2	88.6±1.2	92.3±1.0	55.3±7.5	56.7
DMoN	X, A	70.1±3.8	54.9±4.6	70.2±4.0	86.7±2.4	74.8±5.8	89.7±0.7	90.9±1.8	57.1±1.0	74.3
RS-GNN	X, A	77.3±1.9	62.7±2.3	68.7±2.4	90.6±0.5	83.0±1.6	90.1±0.6	92.4±0.8	56.6±1.2	77.7

**Label coverage:** Once a set of representatives are selected from a dataset, we define a specific class label to be *covered* if at least one of the representatives belongs to that class. We define *label coverage* as the percentage of class labels that are covered by the selected representatives. In Table 5, we report the label coverage results for the baselines and our model when selecting  $k = 2c$  representatives for each dataset. Recall that  $c$  is the number of classes. Overall, we observe that RS-GNN performs well in terms of selecting points that cover all labels with an average of 90.8 across the datasets. An interesting phenomenon can be observed for the Arxiv dataset where RS-GNN has a lower label coverage compared to some of the baselines, but a higher accuracy (cf. main text). We believe this is due to the high label imbalance in this dataset (the largest class has 27321 examples and the smallest has 29 examples). Future work can extend our work to optimizing macro accuracy across classes.

**Ablation study:** We conduct an ablation study to verify the contributions of two components in our model: the joint learning and the CenterNorm. To ablate the joint learning, we train our model in three steps: first compute DGI embeddings, then normalize the computed embeddings using CenterNorm, and finally train the clustering part of the loss function on fixed normalized embeddings. To ablate CenterNorm, we run our model under two settings: (1) we do not normalize (we refer to this as “NoNorm”), and (2) we divide all the values in the embedding matrix by a constant number corresponding to the mean of the  $\ell_2$ -norms of the embeddings (we refer to this as “ConstNorm”). The results of the ablation study are presented in Table 6. Notice that our model benefits from both joint learning and CenterNorm. We also observe that CenterNorm is more effective than ConstNorm. As explained in Section 5.3, we believe this is because the per-node  $\ell_2$  normalization of CenterNorm helps bring the nodes within one cluster closer to each other which helps in identifying clusters and selecting representatives.

## B Proof of the Theorem

**Theorem B.1.** *There is no polynomial-time representative selection algorithm for FoN with an approximation factor better than  $\omega(n^{-1/\text{poly} \log \log n})$ , unless the exponential-time hypothesis fails.*

We start with two lemmas before proceeding to prove this result. We use  $(i, j)$  to represent a data point in the FoN problem with value 1 on features  $i$  and  $j$ .

**Lemma B.2.** *Let  $S$  be the set of data points selected by an RS algorithm. Let  $(i, j)$  be a data point such that for all  $t$  we have  $(i, t) \notin S$ , or for all  $t$  we have  $(t, j) \notin S$ . Then the label of  $(i, j)$  is independent of the labels of  $S$ .*

*Proof.* Let  $S$  be the set of data-points selected by an RS algorithm. Let  $(i, j)$  be a data-point such that for all  $t$  we have  $(i, t) \notin S$ . This means that the labels of data-points in  $S$  are independent of the type of feature  $i$ . Recall that the type of feature  $i$  is chosen independently and uniformly at random. Hence, conditioned on the labels in  $S$ , the label of  $(i, j)$  is 0 with probability  $1/2$  and 1 with probability  $1/2$ . Similar argument holds when for all  $t$  we have  $(t, j) \notin S$ .  $\square$

Table 5: Label coverage of different RS algorithms when  $k = 2c$ .

Selector	Context	Cora	CiteSeer	Pubmed	Photos	PC	CS	Physics	Arxiv	Avg.
Random	—	86.4±10.8	84.2±12.7	85.0±17.0	80.6±11.1	64.0±9.4	72.7±9.4	75.0±14.3	55.0±4.9	75.4
Popular	<b>A</b>	85.7±0.0	50.0±0.0	66.7±0.0	37.5±0.0	30.0±0.0	66.7±0.0	20.0±0.0	15.0±0.0	46.4
KMedoid	<b>X</b>	100.0±0.0	100.0±0.0	66.7±0.0	87.5±0.0	80.0±0.0	73.3±0.0	60.0±0.0	50.0±0.0	77.2
KMeans	<b>X</b>	100.0±0.0	83.3±0.0	100.0±0.0	75.0±0.0	70.0±0.0	46.7±0.0	60.0±0.0	65.0±0.0	75.0
FFS	<b>X</b>	84.3±11.3	88.3±9.5	71.7±12.2	93.1±8.6	74.5±9.4	36.3±3.4	67.0±9.8	63.0±2.3	72.3
MC (RBF)	<b>X</b>	100.0±0.0	100.0±0.0	66.7±0.0	75.0±0.0	60.0±0.0	66.7±0.0	60.0±0.0	52.5±0.0	72.6
MC (cos)	<b>X</b>	97.1±5.9	98.3±5.1	100.0±0.0	75.0±0.0	80.0±0.0	66.7±0.0	100.0±0.0	55.2±0.8	84.0
KMedoid	<b>DGI</b>	79.3±11.8	58.3±10.1	93.3±13.7	100.0±0.0	80.0±9.2	83.7±7.0	87.0±14.9	OOM	—
KMeans	<b>DGI</b>	100.0±0.0	90.0±8.4	100.0±0.0	96.9±5.5	82.5±6.4	99.3±2.0	100.0±0.0	54.2±5.0	90.4
FFS	<b>DGI</b>	96.4±6.3	86.7±10.3	66.7±18.7	77.5±7.7	65.0±6.1	97.0±3.4	95.0±8.9	52.0±5.1	79.5
MC (RBF)	<b>DGI</b>	71.4±0.0	81.7±5.1	66.7±0.0	75.0±0.0	60.0±0.0	52.0±4.6	85.0±8.9	28.1±4.0	65.0
MC (cos)	<b>DGI</b>	100.0±0.0	100.0±0.0	100.0±0.0	87.5±0.0	82.5±5.5	93.7±1.5	85.0±11.0	37.5±2.4	85.8
MinCUT	<b>X, A</b>	78.6±8.7	83.3±15.3	95.0±12.2	12.5±0.0	10.0±0.0	85.7±5.0	99.0±4.5	42.2±4.6	63.3
DMoN	<b>X, A</b>	90.0±9.4	90.0±10.0	91.7±14.8	87.5±5.7	76.0±9.9	90.3±4.6	97.0±7.3	60.2±6.3	85.3
RS-GNN	<b>X, A</b>	100.0±0.0	90.0±8.4	100.0±0.0	98.8±3.9	82.5±9.7	100.0±0.0	100.0±0.0	54.8±3.6	90.8

Table 6: Ablation study results for RS-GNN.

Ablation	Cora	CiteSeer	PubMed	Photos	PC	CS	Physics	Avg.
NoNorm	61.6±7.7	41.5±3.5	59.6±4.7	82.5±2.1	71.3±2.8	86.6±2.4	90.8±1.5	70.6
ConstNorm	59.3±6.9	44.3±4.2	61.7±3.9	84.2±1.4	75.0±3.1	86.7±1.3	90.5±2.1	71.7
NotJoint	71.6±2.9	54.2±3.8	62.8±3.6	84.9±2.5	73.8±3.1	88.2±1.6	91.0±1.7	75.2
Full Model	71.8±3.0	54.7±3.9	65.8±3.0	86.3±1.4	74.3±1.7	89.3±0.8	90.0±2.6	76.0

**Lemma B.3.** Let  $(i_0, i_1), (i_1, i_2), (i_2, i_3), \dots, (i_{l-1}, i_l)$  be a sequence of data points such that for all  $t \in \{1, \dots, l\}$  we have  $(i_{t-1}, i_t) \in \mathcal{S}$ . Given the labels of the data points in  $\mathcal{S}$  we can infer the label of  $(i_0, i_l)$ .

*Proof.* Consider two data-points  $(i, j)$  and  $(j, t)$ . If the labels of both data-points are 1, it means that features  $i, j$  and  $t$  have the same type. Hence, the label of  $(i, t)$  is 1 too. If the labels of both of them are 0, it means that the type of features  $i$  and  $j$  are different, and the type of features  $j$  and  $t$  are different. Hence, the type of features  $i$  and  $t$  are the same, which means the label of  $(i, t)$  is 1. A similar argument shows that if either  $(i, j)$  or  $(j, t)$  has label 1 and the other has label 0, then the label of  $(i, t)$  is 0. Thus, knowing the labels of  $(i, j)$  and  $(j, t)$  determines the label of  $(i, t)$ . Applying this inductively proves the lemma.  $\square$

*Proof of Theorem 4.2.* The proof goes by reducing the densest  $k$ -subgraph problem to the FoN problem. In the densest  $k$ -subgraph problem, we have an unweighted graph  $\mathbb{G}$ , and the goal is to find a subgraph of  $\mathbb{G}$  with  $k$  vertices and the maximum number of edges. We say an algorithm is an  $\alpha$ -approximation algorithm for the densest  $k$ -subgraph problem if it returns a subgraph with  $k$  vertices where the number of edges is at least  $\alpha$  times that of the densest  $k$ -subgraph. It is known that there is no  $\omega(n^{-1/\text{poly log log } n})$ -approximation polynomial-time algorithm for the densest  $k$ -subgraph problem unless ETH fails [46].

Next, we show how to transform an input of the densest  $k$ -subgraph problem to an input to the FoN problem, and then show how to transform an approximate solution for the FoN problem to an approximate solution for the densest  $k$ -subgraph problem while only increasing the approximation factor by a constant. Therefore an  $\omega(n^{-1/\text{poly log log } n})$ -approximation polynomial-time algorithm for the FoN implies an  $\omega(n^{-1/\text{poly log log } n})$ -approximation polynomial-time algorithm for the densest  $k$ -subgraph problem, which does not exist unless ETH fails.

Let  $\mathbb{G} = (V, E)$  be an input to the densest  $k$ -subgraph problem.<sup>4</sup> For each vertex in  $\mathbb{G}$  we define a feature and for each edge in  $\mathbb{G}$  we construct a data point. For each data point corresponding to an edge  $(u, v)$ , the value of the features corresponding to vertices  $u$  and  $v$  are 1 and the value of all other features are 0. As defined in the FoN problem the type (red or blue) of each feature is chosen independently and uniformly at random.

Let  $\mathbb{H} = (V_{\mathbb{H}}, E_{\mathbb{H}})$  be a densest  $k$ -subgraph of  $\mathbb{G}$  and let  $\mathbb{F}$  be a maximal spanning forest of  $\mathbb{H}$ . Note that since there is no cycle in  $\mathbb{F}$ , the number of edges in  $\mathbb{F}$  is at most  $k - 1$ . Moreover, since  $\mathbb{F}$  is a maximal forest of  $\mathbb{H}$ , for each edge  $e$  in  $\mathbb{H}$ , there is a path between the endpoints of  $e$  in  $\mathbb{F}$  (otherwise we could add  $e$  to  $\mathbb{F}$ ). Hence, if we query the data points corresponding to the edges of  $\mathbb{F}$ , by Lemma B.3, we can determine the label of all the edges in  $\mathbb{H}$ , which is an  $\frac{|E_{\mathbb{H}}|}{|E|}$  fraction of all data points. This gives us a solution with  $\overline{\text{Acc}} \geq \Omega\left(\frac{|E_{\mathbb{H}}|}{|E|}\right)$ .

Let  $\mathcal{S}$  be the set of data points selected by an  $\alpha$ -approximation RS algorithm, and  $V_{\mathcal{S}}$  be the set of vertices adjacent to the edges corresponding to the data points in  $\mathcal{S}$ . By Lemma B.2, if the edge corresponding to a data point has one (or two) endpoints in  $V \setminus V_{\mathcal{S}}$ , then the label of that data point is independent of the labels of  $\mathcal{S}$ . Hence, the number of data points whose label is not independent of the labels in  $\mathcal{S}$  is at most the number of edges induced by  $V_{\mathcal{S}}$ . We denote this edge set by  $E_{\mathcal{S}}$ . Recall that  $\mathcal{S}$  is an  $\alpha$ -approximate solution, i.e.,  $|E_{\mathcal{S}}| = \Omega(\alpha|E_{\mathbb{H}}|)$ . On the other hand,  $|\mathcal{S}| \leq k$  and hence  $|V_{\mathcal{S}}| \leq 2k$ . One can decompose the induced subgraph of  $V_{\mathcal{S}}$  into  $\binom{4}{2} = 6$  subgraphs each with  $k$  vertices, and pick the one with the maximum number of edges. This gives an  $\Omega(\alpha)$ -approximate solution to the densest  $k$ -subgraph problem.  $\square$

## C DGI & CenterNorm

With the joint loss function used in the main text, the model can trivially reduce  $\mathcal{L}_{\text{SEL}}$  by making the values in the embedding matrix  $\mathbf{H}$  arbitrarily small. That is because multiplying a small constant to  $\mathbf{H}$  may not change  $\mathcal{L}_{\text{EMB}}$  substantially, but it can make the distances between the nodes arbitrarily small, resulting in a low value for  $\mathcal{L}_{\text{SEL}}$  even for a random representative embedding matrix  $\mathbf{R}$ .

One way to avoid the aforementioned problem is by normalizing the embedding matrix  $\mathbf{H}$  before using it for selection. However, one should be careful about the choice of the normalization to avoid losing useful information. Before explaining how we normalize the embeddings, we describe a property of DGI embeddings that motivates our normalization.

Figure 3 shows a UMAP plot of the DGI embeddings  $\mathbf{H}$  for the nodes in the original graph of Cora and the embeddings  $\mathbf{H}'$  for the nodes in a corrupted Cora graph (red). It can be observed that the  $\mathbf{H}'$  embeddings form a large cluster that is mostly in between the  $\mathbf{H}$  embeddings. The  $\mathbf{H}$  embeddings form small size clusters that are placed around the large cluster of  $\mathbf{H}'$ . To understand why this happens, notice that when we shuffle the node features for creating corrupted graphs for DGI training, the node features of the neighbors of each node are a random subsample of the node features in the graph. Therefore, the GNN aggregation function applied on the projected node embeddings makes the embeddings go toward the mean of projected embeddings. This makes the corrupted node embeddings  $\mathbf{H}'$  form a large cluster in the middle and the embeddings  $\mathbf{H}$  be placed outside and around this cluster.

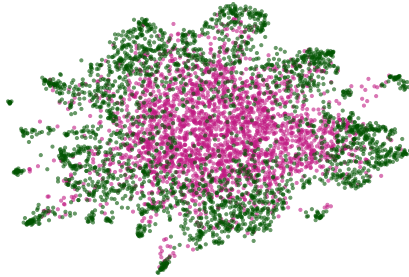


Figure 3: A UMAP plot of the DGI node embeddings for the nodes in the original graph of Cora (green) and the nodes in a corrupted Cora graph (red).

Besides visual inspection, we also cluster the node embeddings  $\mathbf{H}$  for Cora into 7 clusters using KMeans (7 is the number of classes in Cora; this provides good clusters with a normalized mutual information of 55.95 with the node labels). Then we compute the distance between each cluster

<sup>4</sup>Note that graph  $\mathbb{G}$  is not an attributed graph, rather a simple graph which is an input to the densest  $k$ -subgraph problem.



Table 7: Dataset statistics.

Dataset	Nodes	Edges	Features	Classes
Cora	2,708	5,278	1433	7
CiteSeer	3,312	4,536	3703	6
Pubmed	19,717	44,324	500	3
Amazon Photo	7,650	119,081	745	8
Amazon PC	13,752	245,861	767	10
Coauthor CS	18,333	81,894	6,805	15
Coauthor PHY	34,493	247,962	8,415	5
OGBN-Arxiv	169,343	1,157,799	128	40

center and the mean of these centers and obtain the following seven distances: 1.4, 1.2, 1.3, 1.2, 0.6, 1.4, 1.5. All cluster centers are at a good distance from the mean and, with the exception of one cluster, they are at a similar distance from the mean. We then subtract the mean and compute the angle between the cluster centers. We observe that the minimum angle between two cluster centers is 60.1 degrees and the average angle is 76.6 degrees.

The above analysis motivates the CenterNorm normalization outlined in the main text. Furthermore, the analysis shows that DGI is a good candidate for RS as it groups data points into small-sized dense clusters in the latent space, thus an RS algorithm can select representatives from each dense cluster.

## D Datasets

We used eight established benchmarks in the GNN literature. The first three datasets are Cora, CiteSeer, and Pubmed [55, 34]. These datasets are citation networks in which nodes represent papers, edges represent citations, features are bag-of-word abstracts, and the labels represent paper topics. The next two datasets are Amazon Photo and Amazon PC [57]. These two datasets correspond to photo and computers subgraphs of the Amazon copurchase graph. In these graphs, the nodes represent goods with an edge between two nodes representing that they have been frequently purchased together. Node features are bag-of-word reviews and class labels are product categories. The next two datasets are Coauthor CS and Coauthor Physics [57]. These are co-authorship networks for the computer science and physics fields based on the Microsoft Academic Graph respectively. The nodes in these two datasets represent authors, edges represent co-authorship, node features are a collection of paper keywords from author’s papers, and the class labels are the most common fields of study. Our last dataset is OGBN-Arxiv [34] which is also a citation dataset similar to Cora, CiteSeer, and Pubmed, but orders of magnitude bigger than the three. The features in this dataset are average word embeddings of the paper abstracts.

A summary of our dataset statistics are provided in Table 7.

## E Implementation Details

We implemented our model and the baselines in Jax/Flax [9, 31] and used the Jraph library [27] for our GNN operations. Our experiments were done on a JellyFish TPU for all datasets except for the Arxiv dataset where we used a DragonFish TPU as the experiments with the Arxiv dataset require more memory. For our DGI model, we used a single-layer GCN model with SeLU activations [40]. For the experiments that had access to the original graph structure, we set the DGI hidden dimension to 512 for all datasets except for the Arxiv dataset where we set it to 256 to reduce memory usage. For the experiments with no access to the original graph structure, we set the DGI hidden dimension to 128 as there exists less signal in this case. We trained the DGI models for 2000 epochs both for our model and the baselines. For KMeans and KMedoid, we used the implementation in scikit-learn [52] and scikit-learn-extra<sup>5</sup> respectively. To reduce the quadratic time complexity of MaxCover, we apply MaxCover on a k-nearest neighbors similarity graph in the input features/embeddings as opposed to the full graph. We used different hyperparameters for the RBF kernel (in the case of MaxCover

<sup>5</sup><https://github.com/scikit-learn-contrib/scikit-learn-extra>

with RBF similarities) and kNN and reported the values that resulted in the best overall accuracy across models. For MinCUT and DMoN, we used the implementation from the DMoN paper. For our model, we set  $\lambda$  in the main loss function to 0.001 for all datasets. Also, for the experiments where a graph structure is not provided as input, to create a kNN graph we connect each node to its closest 15 nodes for all the datasets.

For the classification GCN model, we used a two-layer GCN model with PReLU activations [30] and with a hidden dimension of 32. We added a dropout layer after the first layer with a drop rate of 0.5. The weight decay was set to  $5e^{-4}$ . The GCN is trained based on the nodes in the selected set  $\mathcal{S}$  of representatives. We randomly split the remaining nodes in  $(\mathcal{V} - \mathcal{S})$  into validation and test sets by selecting 500 nodes for validation and the rest for testing.

We ran all the experiments 20 times (except for Arxiv where we ran it 10 times) with different random seeds and reported the mean and standard deviation of the runs.